# Dianion of Pyrrole-2-*N*-(*o*-hydroxyphenyl)carbaldimine as an Interesting Tridentate (ONN) Ligand System in Hypercoordinate Silicon Complexes

Daniela Gerlach,[†] Erica Brendler,[‡] Thomas Heine,[§] and Jörg Wagler*[,†]

*Institut für Anorganische Chemie and Institut für Analytische Chemie, Technische Universität Bergakademie Freiberg, Leipziger Strasse 29, D-09596 Freiberg, Germany, and Institut für Physikalische Chemie und Elektrochemie, Technische Universität Dresden, Mommsenstrasse 13, D-01062 Dresden, Germany*

*Received September 22, 2006*

The tridentate title ligand was found to act as an ($N_{eq}N_{ax}O_{eq}$) = ($N_{amide}$,$N_{imine}$,$O_{phenolate}$) ligand as well as an ($N_{ax}N_{eq}O_{ax}$) ligand in pentacoordinate silicon complexes depending on the substituents at the Si atom. Its two notably different coordination modes in ($N_{eq}N_{ax}O_{eq}$)Si($CH_2$)$_3$ and ($N_{ax}N_{eq}O_{ax}$)SiPhMe were studied with X-ray structure analysis as well as $^{29}$Si CP/MAS NMR spectroscopy together with quantum chemical calculations of geometry and NMR chemical shielding tensors.

## Introduction

Hypercoordinate silicon complexes attract chemists' interest from various points of view: Enhanced reactivities of silicon complexes due to increased coordination numbers[1] as well as modified electronic properties as result of modified ligand spheres and coordination geometries[2] represent only a small extract of specialties that are provided by hypercoordinate Si complexes.[3] The tendency of the Si atom to coordinate to more than four donor atoms, however, is remarkably influenced by the electron-releasing and -withdrawing character of its substituents. Thus, hypercoordinate complexes of dialkylsilanes with less Lewis acidic Si central atoms are scarcely encountered in the literature,[4] while halosilanes are likely to attract further donors.[5] In order to achieve hypercoordination at the Si atom, various kinds of chelating ligands are applied. Kost et al. extensively studied the electronic influences of remote substituents at carboxylic hydrazide-derived bidentate (ON) ligand systems,[6] silicates bearing (OO) ligands of diolate type are known from studies of Tacke et al. and other groups,[7] and even (NN) chelating systems such as 2,2′-bipyridine[8] and 1,10-phenanthroline[9] were successfully applied to prepare hypercoordinate silicon complexes. Unlike these, silicon complexes of tridentate chelating ligand systems are almost unexplored. Recently, Tacke et al. published studies on Si complexes of the (ONO) ligand system derived from acetylacetone and *o*-aminophenol (Scheme 1),[10] Böhme et al. presented first insights into Si complexes of chiral (ONO) ligands,[11] and Gómez et al. and Prakasha et al. also investigated Si complexes of (ONO) ligand systems of pyridine-2,6-dimethanols and -diethanols (Scheme 1).[12] Furthermore, some examples of silicon (NNN) chelates are known from the work of Boudjouk et al. (Scheme 1).[13]

The notable lack of Si complexes bearing an (NNO) ligand system, crystal structures of which have not been published so

* Corresponding author. Tel: (+49) 3731 39 3556 or (+49) 3731 39 4343. Fax: (+49) 3731 39 4058. E-mail: joerg.wagler@chemie.tu-freiberg.de.

† Institut für Anorganische Chemie, Technische Universität Bergakademie Freiberg.

‡ Institut für Analytische Chemie, Technische Universität Bergakademie Freiberg.

§ Institut für Physikalische Chemie und Elektrochemie, Technische Universität Dresden.

(1) (a) Chuit, C.; Corriu, R. J. P.; Reye, C.; Young, J. C. *Chem. Rev.* **1993**, *93*, 1371. (b) Dilman, A. D.; Ioffe, S. L. *Chem. Rev.* **2003**, *103*, 733. (c) Denmark, S. E.; Sweis, R. F. *Acc. Chem. Res.* **2002**, *35*, 835. (d) Wagler, J.; Doert, T.; Roewer, G. *Angew. Chem., Int. Ed.* **2004**, *43*, 2441. (e) Wagler, J.; Böhme, U.; Roewer, G. *Organometallics* **2004**, *23*, 6066. (f) Kira, M.; Zhang, L. C.; Kabuto, C.; Sakurai, H. *Organometallics* **1996**, *15*, 5335.

(2) (a) Wagler, J.; Gerlach, D.; Böhme, U.; Roewer, G. *Organometallics* **2006**, *25*, 2929. (b) Yamaguchi, S.; Akiyama, S.; Tamao, K. *J. Organomet. Chem.* **2002**, *652*, 3.

(3) (a) Kost, D.; Kalikhman, I. *Adv. Organomet. Chem.* **2004**, *50*, 1. (b) Tacke, R.; Pülm, M.; Wagner, B. *Adv. Organomet. Chem.* **1999**, *44*, 221.

(4) (a) Karsch, H. H.; Richter, R.; Witt, E. *J. Organomet. Chem.* **1996**, *512*, 185. (b) Zheng, J.-Y.; Konishi, K.; Aida, T. *Inorg. Chem.* **1998**, *37*, 2591. (c) Hensen, K.; Gebhardt, F.; Bolte, M. *Z. Anorg. Allg. Chem.* **1997**, *623*, 633. (d) Gostevskii, B.; Kalikhman, I.; Tessier, C. A.; Panzner, M. J.; Youngs, W. J.; Kost, D. *Organometallics* **2005**, *24*, 5786. (e) Kalikhman, I.; Gostevskii, B.; Botoshansky, M.; Kaftory, M.; Tessier, C. A.; Panzner, M. J.; Youngs, W. J.; Kost, D. *Organometallics* **2006**, *25*, 1252.

(5) (a) Nakash, M.; Goldvaser, M. *J. Am. Chem. Soc.* **2004**, *126*, 3436. (b) Knopf, C.; Herzog, U.; Roewer, G.; Brendler, E.; Rheinwald, G.; Lang, H. *J. Organomet. Chem.* **2002**, *662*, 14. (c) Hensen, K.; Stumpf, T.; Bolte, M.; Näther, C.; Fleischer, H. *J. Am. Chem. Soc.* **1998**, *120*, 10402. (d) Kano, N.; Komatsu, F.; Kawashima, T. *J. Am. Chem. Soc.* **2001**, *123*, 10778.

(6) (a) Gostevskii, B.; Silbert, G.; Adear, K.; Sivaramakrishna, A.; Stalke, D.; Deuerlein, S.; Kocher, N.; Voronkov, M. G.; Kalikhman, I.; Kost, D. *Organometallics* **2005**, *24*, 2913. (b) Kost, D.; Kingston, V.; Gostevskii, B.; Ellern, A.; Stalke, D.; Walfort, B.; Kalikhman, I. *Organometallics* **2002**, *21*, 2293.

(7) (a) Sahai, N.; Tossell, J. A. *Inorg. Chem.* **2002**, *41*, 748. (b) Benner, K.; Klüfers, P.; Vogt, M. *Angew. Chem., Int. Ed.* **2003**, *42*, 1058. (c) Pak, J. J.; Greaves, J.; McCord, D. J.; Shea, K. J. *Organometallics* **2002**, *21*, 3552. (d) Tacke, R.; Burschka, C.; Richter, I.; Wagner, B.; Willeke, R. *J. Am. Chem. Soc.* **2000**, *122*, 8480.

(8) (a) Kummer, D.; Chaudhry, S. C.; Thewalt, U.; Debaerdemaeker, T. *Z. Anorg. Allg. Chem.* **1987**, *553*, 147. (b) Hensen, K.; Mayr-Stein, R.; Ruhl, S.; Bolte, M. *Acta Crystallogr., Sect. C* **2000**, *56*, 607.

(9) (a) Kummer, D.; Chaudhry, S. C.; Depmeier, W.; Mattern, G. *Chem. Ber.* **1990**, *123*, 2241. (b) Nakash, M.; Goldvaser, M.; Goldberg, I. *Inorg. Chem.* **2004**, *43*, 5792.

(10) Seiler, O.; Burschka, C.; Metz, S.; Penka, M.; Tacke, R. *Chem.−Eur. J.* **2005**, *11*, 7379.

(11) Böhme, U.; Wiesner, S.; Günther, B. *Inorg. Chem. Commun.* **2006**, *9*, 806.

(12) (a) Prakasha, T. K.; Chandrasekaran, A.; Day, R. O.; Holmes, R. R. *Inorg. Chem.* **1996**, *35*, 4342. (b) Gómez, E.; Santes, V.; de la Luz, V.; Farfán, N. *J. Organomet. Chem.* **1999**, *590*, 237. (c) Gómez, E.; Santes, V.; de la Luz, V.; Farfán, N. *J. Organomet. Chem.* **2001**, *622*, 54.

(13) (a) Kim, B.-K.; Choi, S.-B.; Kloos, S. D.; Boudjouk, P. *Inorg. Chem.* **2000**, *39*, 728. (b) Choi, S.-B.; Kim, B.-K.; Boudjouk, P.; Grier, D. G. *J. Am. Chem. Soc.* **2001**, *123*, 8117.

10.1021/om060869b CCC: $37.00 
Publication on Web 12/06/2006

**Scheme 1**

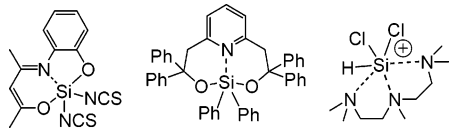

**Scheme 2**

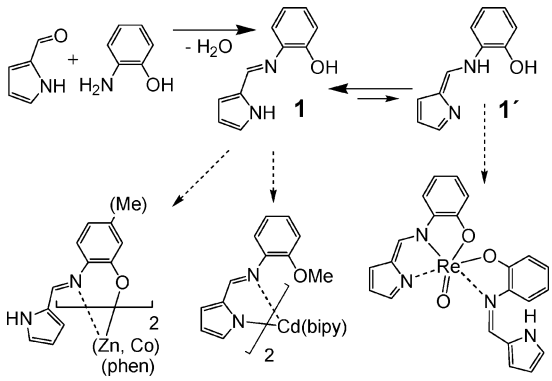

far, was reason enough to explore this new field of silicon coordination chemistry using pyrrole-2-*N*-(*o*-hydroxyphenyl)-carbaldimine[14] (**1**) (Scheme 2) as a bifunctional tridentate ligand system bearing three different kinds of donor functions. This ligand and systems derived thereof were already applied in transition metal complex chemistry and proved to exhibit different bi- and tridentate coordination modes. In complexes of Zn,[15] Co,[16] and Cd[17] this ligand acts as a bidentate ($N_{imine}O_{phenolate}$) and ($N_{amide}N_{imine}$) system related to the tautomer depicted in Scheme 2, left, with a short M−N distance to the pyrrole N atom and a significantly longer M−N′ distance to the imine N atom in case of the cadmium complex. A rhenium complex by Sawusch et al.[14] revealed the general possibility of this tridentate ligand system to exhibit the coordination behavior of the dianion derived from the tautomer depicted in Scheme 2, right. While these different coordination patterns might depend on the different central transition metal ions, in our study extremely different tridentate coordination modes, which refer to the two different tautomeric forms of **1**, were found in two silicon complexes.

## Results and Discussion

According to Scheme 2, ligand **1** was prepared by condensation of pyrrole-2-carbaldehyde with *o*-aminophenol in ethanol. Its molecular structure was determined by single-crystal X-ray diffraction (Figure 1, Table 2).

Bond lengths of **1** are listed in Table 1. Hydrogen atoms H1a and H1b were detected by analysis of the residual electron density and refined without bond length restraints. H1a is undoubtedly attached to the phenol oxygen atom O1 [O1−H1a 0.86(2) Å] and H1b to the pyrrole atom N1 [N1−H1b 0.91(1) Å]. H1a is situated within a hydrogen bridge between O1 and N2; the bond length C11−O1 [1.372(1) Å], however, clearly

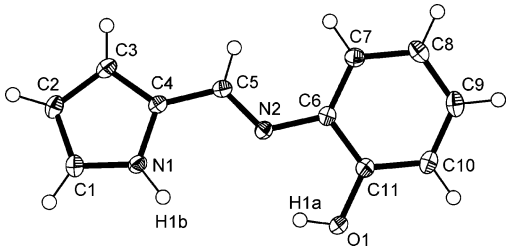

**Figure 1.** Molecular structure of **1** in the crystal (ORTEP plot with 50% probability ellipsoids).

demonstrates the presence of the phenolic hydroxy group. The bond length of the imine moiety C5═N2 [1.283(1) Å] represents an unaltered C═N double bond, and all of the interatomic distances from N1 to C5 agree with the tautomeric form **1**.

Reaction of **1** with 1,1-dichlorosilacyclobutane and methylphenyldichlorosilane resulted in the formation of the pentacoordinate silicon complexes **2** and **3**, respectively (Scheme 3).

As already indicated in Scheme 3, the X-ray structures of complexes **2** and **3** (Figures 2 and 3) exhibit notable structural differences between these molecules, which require the discussion of different electronic states of the tridentate ligand while coordinating the silicon atoms. (Compound **2** was found to crystallize in two modifications: monoclinic $P2_1$, $Z = 4$, from chloroform at room temperature; orthorhombic $Pca2_1$, $Z = 8$, from diethyl ether at −21 °C. Because of similar molecular conformations of **2** in both modifications, only the orthorhombic structure is discussed.) Each of the crystal structures bears two crystallographically independent molecules, but there are no significant differences in the bond lengths and only small deviations in the angles between the two molecules of each pair. Therefore, only one molecule of each of the compounds **2** and **3** is discussed further as a representative example.

The Si atom of **2** is situated in a distorted trigonal bipyramidal coordination sphere, almost midway between trigonal bipyramid (TBP) and square pyramid (SQP): 57% TBP with the imine nitrogen atom N2 and a silacyclobutane carbon atom (C12) in axial positions [angle N2−Si1−C12 175.3(1)°]. The other donor atoms (N1, O1, and C14) occupy equatorial sites. (The progress between TBP and SQP coordination geometry, % TBP, was determined using the equation % TBP = 100% (Angle 1 − Angle 2)/60°, in which Angle 1 is the widest angle X−Si−Y within the pentacoordinate geometry, i.e., the axial angle, and Angle 2 is the widest angle in the equatorial plane with respect to the axis defined with Angle 1. This general equation was derived from the special form % TBP = 100% (|Angle N−Si−N − Angle O−Si−O|)/60°, which has been used by Kost et al.[6b]) Owing to the axial situation of C12, the bond Si1−C12 [1.904(2) Å] is slightly longer than Si1−C14 [1.871(2) Å]. The lengths of the Si−N bonds, however, exhibit notable differences [Si1−N1 1.840(2) Å, Si1−N2 1.954(1) Å]. The C═N double bond of the imine moiety is slightly stretched [C5═N2 1.299(2) Å].

Contrasting this coordination pattern of the tridentate ligand system, **3** exhibits completely different structural features.

In **3** the pentacoordinate Si atom is also surrounded by distorted trigonal bipyramidally arranged donor atoms, again almost midway between TBP and SQP (43% TBP). In this complex, however, the axial positions are occupied by the donor atoms N1 and O1 [angle N1−Si1−O1 160.82(7)°]. The initial imine donor atom N2 occupies an equatorial site (together with the carbon atoms C12 and C18). This ($N_{ax}N_{eq}O_{ax}$) coordination motif of the tridentate ligand results in further crucial differences between **2** and **3**: Si1−N2 [1.897(1) Å] is significantly shorter

(14) Sawusch, S.; Jäger, N.; Schilde, U.; Uhlemann, E. *Struct. Chem.* **1999**, *10*, 105.

(15) (a) Castro, J. A.; Romero, J.; Garcia-Vazquez, J. A.; Sousa, A.; Castellano, E. E.; Zuckerman-Schpector, J. *J. Coord. Chem.* **1993**, *30*, 165. (b) Castro, J. A.; Romero, J.; Garcia-Vazquez, J. A.; Macias, A.; Sousa, A.; Englert, U. *Polyhedron* **1993**, *12*, 1391.

(16) Castro, J. A.; Romero, J.; Garcia-Vazquez, J. A.; Sousa, A.; Castiñeiras, A. *J. Chem. Cryst.* **1994**, *24*, 469.

(17) Castro, J. A.; Romero, J.; Garcia-Vazquez, J. A.; Sousa, A.; Castellano, E. E.; Zuckerman-Schpector, J. *Polyhedron* **1993**, *12*, 31.

**Table 1. Bond Lengths *d* [Å] within the Tridentate Ligand Moiety of 1, 2, and 3 (data of one representative molecule in the case of compounds 2 and 3, respectively)**

| bond | **1** *d* [Å] | **2** *d* [Å] | **3** *d* [Å] | bond | **1** *d* [Å] | **2** *d* [Å] | **3** *d* [Å] |
|---|---|---|---|---|---|---|---|
| N1−C1 | 1.359(1) | 1.359(2) | 1.352(3) | N2−C6 | 1.406(1) | 1.394(2) | 1.396(2) |
| C1−C2 | 1.375(2) | 1.390(3) | 1.383(3) | C6−C7 | 1.397(1) | 1.389(2) | 1.377(2) |
| C2−C3 | 1.408(2) | 1.398(3) | 1.376(3) | C7−C8 | 1.389(2) | 1.393(3) | 1.384(3) |
| C3−C4 | 1.385(1) | 1.396(2) | 1.393(3) | C8−C9 | 1.391(2) | 1.395(2) | 1.377(3) |
| N1−C4 | 1.371(1) | 1.385(2) | 1.375(2) | C9−C10 | 1.387(2) | 1.396(2) | 1.381(3) |
| C4−C5 | 1.437(1) | 1.412(2) | 1.389(3) | C10−C11 | 1.389(2) | 1.390(2) | 1.383(3) |
| C5−N2 | 1.283(1) | 1.299(2) | 1.306(2) | C6−C11 | 1.400(1) | 1.403(2) | 1.392(2) |
| | | | | C11−O1 | 1.372(1) | 1.359(2) | 1.344(2) |

**Table 2. Crystal Data and Experimental Parameters for the Crystal Structure Analyses of 1, 2, and 3**

| | **1** (CCDC-621246) | **2** (CCDC-621248) | **2** (CCDC-621245) | **3** (CCDC-621247) |
|---|---|---|---|---|
| empirical formula | $C_{11}H_{10}N_2O$ | $C_{14}H_{14}N_2OSi$ | $C_{14}H_{14}N_2OSi$ | $C_{18}H_{16}N_2OSi$ |
| formula mass, g mol$^{-1}$ | 186.21 | 254.36 | 254.36 | 304.42 |
| collection *T*, K | 93(2) | 296(2) | 90(2) | 296(2) |
| $\lambda$(Mo K$\alpha$), Å | 0.71073 | 0.71073 | 0.71073 | 0.71073 |
| cryst syst | monoclinic | monoclinic | orthorhombic | monoclinic |
| space group | *C*2/c | $P2_1$ | $Pca2_1$ | $P2_1/c$ |
| *a*, Å | 28.2723(14) | 5.9727(5) | 25.2284(6) | 9.3085(3) |
| *b*, Å | 4.7091(2) | 25.413(3) | 5.8708(2) | 16.5473(7) |
| *c*, Å | 17.1055(9) | 8.2155(8) | 16.3026(5) | 20.5981(9) |
| $\beta$, deg | 125.333(2) | 90.328(3) | 90 | 99.077(1) |
| *V*, Å$^3$ | 1857.89(16) | 1247.0(2) | 2414.59(12) | 3133.0(2) |
| *Z* | 8 | 4 | 8 | 8 |
| $\rho_{calcd}$, Mg/m$^3$ | 1.331 | 1.355 | 1.399 | 1.291 |
| *F*(000) | 784 | 536 | 1072 | 1280 |
| $\theta_{max}$, deg | 32.0 | 30.0 | 38.0 | 26.0 |
| no. of collected rflns | 13 790 | 14 606 | 54 421 | 32 273 |
| no. of indep rflns | 3205 | 7168 | 6742 | 6160 |
| $R_{int}$ | 0.0360 | 0.0204 | 0.0522 | 0.0284 |
| no. of rflns used | 3205 | 7168 | 6742 | 6160 |
| no. of params | 133 | 325 | 326 | 397 |
| GOF | 1.041 | 1.021 | 1.052 | 1.045 |
| R1, wR2 ($I > 2\sigma(I)$) | 0.0427, 0.1060 | 0.0361, 0.0867 | 0.0378, 0.0983 | 0.0374, 0.0978 |
| R1, wR2 (all data) | 0.0669, 0.1147 | 0.0471, 0.0916 | 0.0479, 0.1029 | 0.0637, 0.1077 |
| max., min. res electron dens, e Å$^{-3}$ | 0.411, −0.230 | 0.232, −0.185 | 0.715, −0.317 | 0.192, −0.245 |

**Scheme 3**

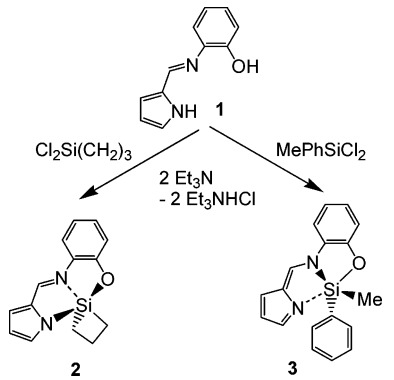


than the distance Si1−N1 [1.923(2) Å]. Although within the limits of the standard error, the "imine" C═N bond of **3** is stretched in comparison with **2** [C5−N2 in **2**: 1.299(2) Å, in **3**: 1.306(2) Å]. The bond lengths within the pyrrole-2-carbaldimine moiety also exhibit slight differences, which are demonstrated in Scheme 4/Table 1 and allow the interpretation of these different coordination modes as a transition from the major influence of one resonance structure to the other one. (Such differences are not found for the iminophenolate moiety C6−C11.)

The ring-strain-release Lewis acidity of silacyclobutanes is expected to be the major reason for the different coordination modes of the tridentate (NNO) ligand in **2** and **3**. Only in a TBP coordination sphere with one carbon atom in axial and one in equatorial position can silacyclobutanes exhibit a lower ring strain. Unlike this, the equatorial situation of both silacyclobutane carbon atoms would increase ring strain. (It is worth mentioning that the conformation of **2** is not locked in solution. The molecules undergo rapid conformational inversion on the NMR time scale, which is indicated by the presence of only two $^{13}$C NMR signals, ratio 2:1, for the silacyclobutane moiety.) Without this ring strain effect, i.e., using monodentate carbon substituents at the Si atom, a transition to the coordination motif depicted in Scheme 4, middle, seems preferred. Taking into account that "equal" bonds are slightly longer in axial than in equatorial positions (compare Si1−C12 and Si1−C14 in **2**), the Si−N bonds in **3** can be considered as "equal" bonds and one cannot distinguish between a longer "dative" and a shorter "covalent" one. Thus, a resonance structure of the tridentate ligand as depicted in Scheme 4, right, seems appropriate to

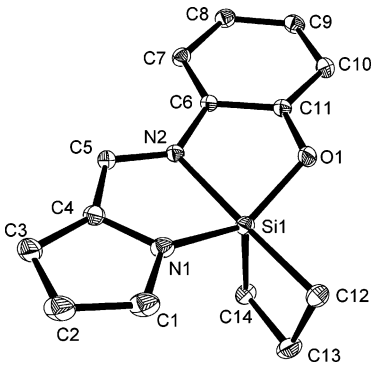


**Figure 2.** Molecular structure of **2** in the crystal (ORTEP plot with 50% probability ellipsoids of one of two crystallographically independent molecules from a crystal of space group $Pca2_1$ at 90 K; hydrogen atoms omitted for clarity).

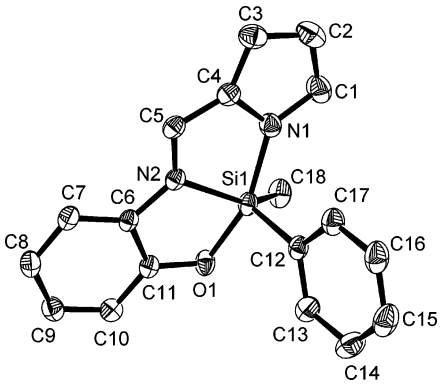


**Figure 3.** Molecular structure of **3** in the crystal (ORTEP plot with 20% probability ellipsoids, one of two crystallographically independent molecules, hydrogen atoms omitted for clarity).

**Scheme 4. Comparison between Selected Bond Lengths of 2 and 3[a] (left and middle) and Suggested Resonance of the Tridentate Dianion Ligand in Complex 3 (right)**

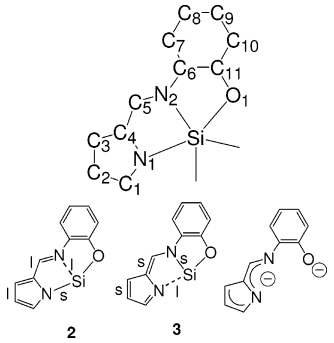


[a] Significantly shorter (s) and significantly longer (l) bonds are indicated by letters as well as bond symbols: (−), (═), and (- - -). Bond symbols (−) and (═) were assigned according to the resonance structure indicated by these bond lengths.

**Scheme 5**

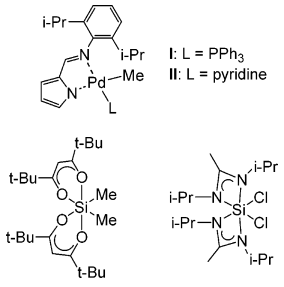


describe this bonding situation. In this case, the delocalization of the negative charge of the pyrrolide anion via two nitrogen donor atoms would account for the preference of this coordination mode in **3**. Related variability of pyrrole-2-carbaldimine ligands has previously been reported by Liang et al.,[18] who described the palladium complexes that are given in Scheme 5, top. **I** exhibits two identical Pd−N bond lengths (about 2.12 Å), and **II** has a significantly longer Pd−$N_{imine}$ bond (2.16 Å) than the Pd−$N_{pyrrolide}$ bond (2.00 Å).

The delocalization of one negative charge within a homobidentate ligand, which results in the formation of two similar bonds between the central atom and the bidentate ligand's donor atoms, has also been encountered with other chelating systems. Hypercoordinate silicon chelates such as acetylacetonato[19] and amidinato[20] ligands are worth mentioning due to a similar kind of negative charge delocalization via two donor atoms of the same atom type (Scheme 5, bottom).

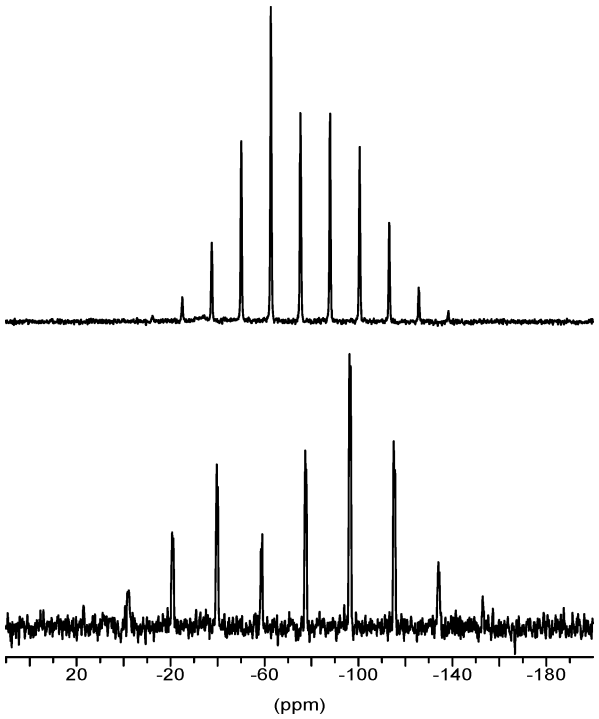


**Figure 4.** $^{29}$Si CP/MAS NMR spectra of **2** ($Pca2_1$), top, and **3**, bottom, at $\nu_{spin}$ = 1 and 1.5 kHz, respectively.

For a deeper insight into the electronic interactions between the tridentate (NNO) ligand system and the Si nuclei in **2** and **3**, the $^{29}$Si NMR shielding tensors were determined by $^{29}$Si CP/MAS NMR spectroscopy and analyzed by comparison with tensors calculated with quantum chemical methods. The calculations were primarily based on the atomic coordinates of the molecules as found by the X-ray structure analyses.

$^{29}$Si CP/MAS NMR spectra of **2** (modification $Pca2_1$) and **3** were recorded at room temperature (Figure 4), and the anisotropic shielding tensors of the respective Si nuclei were determined (Table 3). Two $^{29}$Si NMR signals should arise in each of these solid-state spectra due to the presence of two crystallographically independent molecules in both compounds (see crystal structure analyses). Close structural similarity between the components of each pair of crystallographically unique molecules leads to only one set of signals in the spectrum of **2**. In the case of **3**, two strongly overlapping signals are present. Due to the asymmetric signal broadening as a result of N−Si residual dipolar coupling, the intensities of each of the superimposed isotropic shift signals and spinning side bands were not mathematically separated. The crystal structure of **3** bearing two crystallographically independent but conformationally very similar molecules justifies this simplification.

Modeling of each of the four anisotropic $^{29}$Si NMR shielding tensors (two independent molecules of **2** ($Pca2_1$) and **3**, respectively) using the IGLO method revealed the close $^{29}$Si NMR spectroscopic similarity within each pair of crystallographically independent molecules as well as a good fit of the calculated data with the experimental results for compound **3** (Table 4). In the case of complex **2**, however, the calculations

(18) Liang, H.; Liu, J.; Li, X.; Li, Y. *Polyhedron* **2004**, *23*, 1619.

(19) (a) Xu, C.; Baum, T. H.; Rheingold, A. L. *Inorg. Chem.* **2004**, *43*, 1568. (b) Seiler, O.; Bertermann, R.; Buggisch, N.; Burschka, C.; Penka, M.; Tebbe, D.; Tacke, R. *Z. Anorg. Allg. Chem.* **2003**, *629*, 1403.

(20) Karsch, H. H.; Schlüter, P. A.; Reisky, M. *Eur. J. Inorg. Chem.* **1998**, 433.

**Table 3. Experimental Data of the $^{29}$Si NMR Shielding Tensors of 2 and 3 (without signal separation) as well as the Respective Calculated Data for Both Crystallographically Independent Molecules.**

| | **2** exp | **2** calc | **2** (opt) calc | **3** exp | **3** calc |
|---|---|---|---|---|---|
| $\delta_{11}$/ppm | −31.9 | −27.4/−24.3 | −36.4 | 5.9 | 11.0/11.4 |
| $\delta_{22}$/ppm | −69.7 | −90.2/−96.0 | −68.3 | −100.3 | −102.1/−103.3 |
| $\delta_{33}$/ppm | −124.5 | −126.5/−127.9 | −120.6 | −138.5 | −145.4/141.7 |
| $\delta_{iso}$/ppm | −75.4 | −81.4/−82.7 | −75.1 | −77.4; −77.9 | −78.8/−77.9 |
| Ω/ppm | 92.6 | 99.1/103.6 | 84.2 | 144.4 | 156.4/153.1 |
| $\kappa$ | 0.18 | −0.27/−0.39 | 0.24 | −0.47 | −0.45/−0.50 |

**Table 4. Main Orbital Influences on the Shielding of the $^{29}$Si Nucleus of One Molecule of 2 (atom labels according to the molecular structure of Figure 2)**

| orbital | $\sigma_{11}$ | $\sigma_{22}$ | $\sigma_{33}$ | $\sigma_{iso}$ |
|---|---|---|---|---|
| Si1 (K shell) | 481.7 | 481.7 | 481.7 | 481.7 |
| Si1 (L shell) | 316.9 | 303.9 | 319.0 | 313.3 |
| Si1−N1 | −103.0 | −8.8 | −60.0 | −57.3 |
| Si1−N2 | 2.8 | −81.5 | −52.0 | −43.5 |
| Si1−O1 | −129.8 | −9.0 | −63.1 | −67.3 |
| Si1−C12 | −13.6 | −171.1 | −131.7 | −105.5 |
| Si1−C14 | −189.6 | −133.3 | 6.9 | −105.3 |
| O1 (lone pair) | −5.6 | 2.8 | −6.3 | −3.0 |

**Table 5. Main Orbital Influences on the Shielding of the $^{29}$Si Nucleus of One Molecule of 3 (atom labels according to the molecular structure of Figure 3)**

| orbital | $\sigma_{11}$ | $\sigma_{22}$ | $\sigma_{33}$ | $\sigma_{iso}$ |
|---|---|---|---|---|
| Si1 (K shell) | 481.7 | 481.7 | 481.7 | 481.7 |
| Si1 (L shell) | 294.0 | 315.1 | 325.8 | 311.6 |
| Si1−N1 | −1.3 | −60.4 | −64.1 | −41.1 |
| Si1−N2 | −96.4 | 3.9 | −61.7 | −51.4 |
| Si1−O1 | 2.2 | −85.1 | −90.2 | −57.7 |
| Si1−C12 | −157.1 | −134.0 | −6.0 | −99.0 |
| Si1−C18 | −219.7 | −73.8 | −74.8 | −122.8 |
| O1 (lone pairs) | 4.8 | −4.3 | −3.8 | −1.1 |
| | 0.1 | 0.0 | 0.1 | 0.1 |

based on the crystallographic data produced no satisfactory result. Especially the description of the principal component 22 of the $^{29}$Si NMR tensor appeared to be difficult. Unlike the positive skew in the experimental spectrum, calculations predicted this value to be negative. (The same problem appeared when the crystallographically determined atomic coordinates of **2** in space group $P2_1$ were used as input.) Finally, the $^{29}$Si NMR shift tensor was calculated using the fully optimized molecular geometry of **2**. Surprisingly, the results [**2** (opt) in Table 3] match the experimental data very well, although atomic coordinates were only slightly corrected. Only slight directional changes of the principal components 11 and 33 (due to molecular optimization) may result in notable changes of the direction and shielding properties of the perpendicularly pointing component 22.

The orientations of the principal components of these tensors are demonstrated in Figure 5; only one molecule of each compound is depicted as a representative example.

In Tables 4 and 5 the main orbital influences on the shielding of the respective $^{29}$Si nucleus are listed in the following order: Si atom (core), Si−X bonds (donor atoms), X (lone pairs). A−B bonds (A, B═C, N, O) in closer proximity of the Si atom exhibit only little impact. Generally, the silicon nuclei are shielded by their core electrons (positive $\sigma_{iso}$), and the Si−X bonds to the donor atoms in the first coordination sphere exhibit various deshielding influences (negative $\sigma_{iso}$).

In complex **2** the less shielded direction (11) almost matches the axis N2−Si1−C12 of the trigonal bipyramidal coordination sphere. The deshielding influence of C12 hardly contributes to this direction but does to (22) and (33), the orthogonal components, the same way the bond Si1−C14 mainly contributes to the deshielding in the orthogonal direction (11), contributes less in direction (22), and contributes to the shielding of direction (33). The deshielding impacts of the Si−O and Si−N bonds can be discussed in an analogous manner. The overall isotropic deshielding contributions mainly depend on the donor atom X (increasing deshielding impact: N < O < C) as well as the Si−X bond distance; that is, the isotropic impacts of bonds Si1−C12 and Si1−C14 (similar length) are of similar magnitude, and that of the longer Si1−N2 bond (−43.5) is notably smaller than that of the shorter Si1−N1 bond (−57.3).

As a rough approximation, in compound **3** the less shielded direction (11) also points in the direction of the axis of the trigonal bipyramid (N1−Si1−O1). The generally strong deshielding effects orthogonal to the bond directions are also found for all five bonds to the Si atom in this complex. In spite of the modified site occupations in the bipyramid by the five donor atoms, the general isotropic deshielding impact also decreases from C via O to N. The two different carbon substituents exhibit notably different deshielding behavior; that is, the deshielding influence of the bond to the methyl group (Si1−C18) overcomes that of the bond Si1−C12 to the phenyl substituent. Both effects, the net increased shielding of Si nuclei by replacing methyl for phenyl groups as well as the substituents' influences orthogonal to the bond directions, were also reported for hexacoordinate diorganosilanes.[21]

Unlike in complex **2**, which demonstrates isotropic deshielding influences of the lone pairs of O1, their influence on the (de)shielding of Si1 in complex **3** is negligible. Tacke et al. also studied the (de)shielding influences of the donor atoms in trigonal bipyramidal silicon complexes (Scheme 6).[22] In agreement with our findings, they also observed the axial direction of the TBP coordination sphere as the least shielded direction. Furthermore, Tacke et al. found a strong dependence of the (de)shielding power of lone pairs on their position in the trigonal bipyramid: Lone pairs of axially situated sulfur atoms had a deshielding character, while the equatorially located ones were slightly shielding. Vice versa, lone pairs of oxygen atoms in axial positions were rather shielding than the deshielding ones on equatorial sites. The latter result is similar to our findings of less shielding lone pair impact by an axially located O atom and deshielding action of an equatorially situated O donor atom.

Comparing **2** and **3**, various impacts on the shielding of the $^{29}$Si nuclei can be discussed with respect to the striking structural differences between these two complexes. Due to the presence of two completely different organic substituent patterns, only the impacts of the tridentate ligand system are taken into account for this comparison. The transition from **2** to **3** is accompanied by a lengthening of the Si1−O1 bond (+0.04 Å). Therefore, the net impact of O1 on the electronic deshielding of Si1 decreases. The interconversion of the short and long Si−N bonds

(21) Wagler, J.; Böhme, U.; Brendler, E.; Blaurock, S.; Roewer, G. *Z. Anorg. Allg. Chem.* **2005**, *631*, 2907.

(22) Bertermann, R.; Biller, A.; Kaupp, M.; Penka, M.; Seiler, O.; Tacke, R. *Organometallics* **2003**, *22*, 4104.

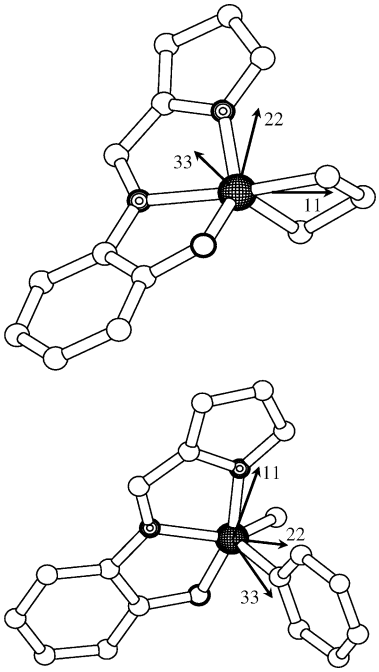


**Figure 5.** Representation of the directions of the principal components of the $^{29}$Si NMR shielding tensor in molecules of **2** (top) and **3** (bottom). Hydrogen atoms were omitted for clarity. The principal components (11), (22), and (33) were assigned with respect to the Herzfeld−Berger notation ($\sigma_{11} < \sigma_{22} < \sigma_{33}$).

**Scheme 6**

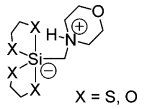


(lengthening of Si1−N1, shortening of Si1−N2) results in a significant change in their deshielding properties. As the bond Si1−N1 has a higher deshielding impact in **2**, the shorter Si−N bond in **3** (Si1−N2) executes a notably stronger deshielding influence than Si1−N1, although the bond length difference is smaller than in the first complex. Thus, the striking increase in the electronic interactions between Si1 and the "imine" nitrogen atom N2 in complex **3** also indicates a transition from one resonance structure of the tridentate ligand ($N_{amide}N_{imine}O$) to the other one ($N_{imine}N_{amide}O$), as depicted in Scheme 4.

## Conclusions

This first structural study on main group element complexes of the tridentate pyrrole-2-*N*-(*o*-hydroxyphenyl)carbaldimine dianion revealed a fascinating flexibility of this ligand regarding (ax,eq,ax) and (eq,ax,eq) coordination modes, the second of which is supported by the ring strain release Lewis acidity of the silacyclobutane moiety. These different site occupations within trigonal bipyramidal coordination spheres lead to [N(pyrrole)→Si, N(imine)−Si] and [N(pyrrole)−Si, N(imine)→Si] bonding patterns. The latter has been found in pyrrole-2-carbaldimine complexes of aluminum (e.g., Scheme 7, left).[23] Longer M−N bonds to the pyrrole moiety versus shorter M−N bonds to the imine N atom have been found only in some transition metal complexes of such ligands (e.g., Scheme 7, right).[24]

**Scheme 7**

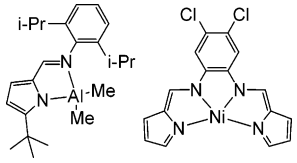


$^{29}$Si NMR spectroscopic studies show that, regardless of the coordination mode of the tridentate chelating system, the less shielded direction in the pentacoordinate Si complexes **2** and **3** corresponds to the axis of the TBP coordination sphere. Therefore, the $^{29}$Si nucleus is well shielded within the equatorial plane. Unlike this, the different substitution patterns of the pentacoordinate Si atoms with (eq,ax) versus (eq,eq) situated carbon atoms, which exert the greatest influence on the $^{29}$Si NMR shielding, lead to notable differences in anisotropy Ω and skew $\kappa$ of the CSA tensor.

Slight structural changes were shown to have enormous influence on solid-state $^{29}$Si NMR spectra. Therefore, small uncertainties or errors in atomic coordinates from X-ray structure analyses may successfully be corrected by quantum chemical optimization to provide a suitable basis for modeling $^{29}$Si NMR shift tensors.

## Experimental Section and Calculations

Syntheses were carried out under an inert atmosphere of dry argon using standard Schlenk techniques and dry solvents. $^{1}$H, $^{13}$C, and $^{29}$Si NMR spectra (solution) were recorded on a Bruker DPX 400 spectrometer using TMS as internal standard. $^{29}$Si CP/MAS spectra were recorded on a Bruker AVANCE 400WB spectrometer using a 7 mm zirconia probe with KelF insert. Chemical shifts are also reported referring to TMS. CSA tensors were obtained from the solid-state spectra using HB-MAS.[25] Melting points were determined in sealed capillaries and not corrected. Single-crystal X-ray structure analyses were carried out on a Bruker-NONIUS X8 APEX2-CCD diffractometer using Mo Kα radiation ($\lambda$ = 0.71073 Å). The structures were solved with direct methods (SHELXS-97) and refined with least-squares method (refinement on $F^2$ against all reflections with SHELXL-97). All non-hydrogen atoms were anisotropically refined. Hydrogen atoms were placed in idealized positions and refined isotropically. Detailed data for the crystal structures of **1**, **2**, and **3** can be found in the Supporting Information.

Atomic coordinates of the X-ray structure of **2** ($Pca2_1$) have been optimized employing gradient-corrected density-functional theory using the hybrid version of the Perdew−Burke−Ernzerhof (PBE)[26] and the 6-31G(d) basis as implemented in Gaussian03.[27] NMR calculations have been performed using density-functional perturbation theory[28,29] with the individual gauge for local orbitals (IGLO)[30] method on electronic structures, which have been calculated at the PBE/IGLO-III[26,31] level using deMon[32] and deMon-NMR.[29] Individual bond contributions correspond to Boys localized molecular orbitals (LMOs).[33]

**Complex 2.** A solution of 1,1-dichlorosilacyclobutane (0.69 g, 4.89 mmol) and triethylamine (1.13 g, 11.2 mmol) in THF (7 mL) was stirred at −10 °C, and a solution of ligand **1**[14] (0.87 g, 4.66 mmol) in THF (7 mL) was added dropwise. Then, the hydrochloride

(23) (a) Liang, L.-C.; Yang, C.-W.; Chiang, M. Y.; Hung, C.-H.; Lee, P.-Y. *J. Organomet. Chem.* **2003**, *679*, 135. (b) Hao, H.; Bhandari, S.; Ding, Y.; Roesky, H. W.; Magull, J.; Schmidt, H. G.; Noltemeyer, M.; Cui, C. *Eur. J. Inorg. Chem.* **2002**, 1060.

(24) (a) Di Bella, S.; Fragala, I.; Guerri, A.; Dapporto, P.; Nakatani, K. *Inorg. Chim. Acta* **2004**, *357*, 1161. (b) Chernyad'ev, A. Y.; Ustynyuk, Y. A.; Aleksandrov, G. G.; Sidorov, A. A.; Novotortsev, V. M.; Ikorskii, V. N.; Nefedov, S. E.; Eremenko, I. L.; Moiseev, I. I. *Russ. Chem. Bull.* **2002**, 1448.

(25) Fenzke, D. *HB-MAS*; Universität Leipzig: Fachbereich Physik, 1989.

(26) Perdew, J. P.; Burke, K.; Ernzerhof, M. *Phys. Rev. Lett.* **1996**, *77*, 3865.

precipitate was filtered and washed with THF (15 mL). The solvent was removed from the filtrate by vacuum condensation, and the solid residue was dissolved in chloroform (3 mL). After 1 min the chloroform was removed under vacuum and the solid residue was extracted with diethyl ether (25 mL). Upon cooling to −21 °C, orange crystals separated out of the ether extract. After 3 days they were filtered and dried in a vacuum. Yield: 0.50 g (1.97 mmol, 42%). Mp: decomposition at 133 °C without melting. $^1$H NMR ($CDCl_3$): $\delta$ 1.3−2.1 (mm, 6H, Si($CH_2$)$_3$), 6.4−7.5 (mm, 7H, Ar), 8.28 (s, 1H, N═CH). $^{13}$C NMR ($CDCl_3$): $\delta$ 13.0 ($CH_2$-*C*$H_2$−$CH_2$), 23.2 (Si−$CH_2$), 113.2, 115.6, 116.7, 119.4, 120.3, 128.5, 129.3, 134.0, 137.8, 143.7 (Ar, C═N), 153.1 (C−O). $^{29}$Si NMR ($CDCl_3$): $\delta$ −76.4. Anal. Calcd for $C_{14}H_{14}N_2OSi$: C, 66.10; H, 5.55; N, 11.01. Found: C, 65.92; H, 5.86; N, 10.92.

**Complex 3.** A solution of methylphenyldichlorosilane (0.43 g, 2.26 mmol) and triethylamine (0.46 g, 4.51 mmol) in THF (5 mL) was stirred at ambient temperature, and a solution of ligand **1**[14] (0.40 g, 2.15 mmol) in THF (5 mL) was added dropwise. The mixture was stored at 4 °C for 30 min, then the hydrochloride precipitate was filtered and washed with THF (12 mL). The solvent was removed from the filtrate by vacuum condensation, the solid residue was dissolved in chloroform (1 mL), and hexane (0.5 mL) was added. Within a few hours crystals formed, which were filtered, washed with 2 mL of a chloroform/hexane mixture (1:7), and dried in a vacuum. Yield: 0.20 g (0.66 mmol, 31%). Mp: 85 °C. $^1$H NMR ($CDCl_3$): $\delta$ 0.74 (s, 3H, Si−$CH_3$), 6.5−7.5 (mm, 12H, Ar), 8.53 (s, 1H, N═CH). $^{13}$C NMR ($CDCl_3$): $\delta$ 5.7 (Si−$CH_3$), 111.8, 114.6, 117.6, 118.0, 120.5, 127.6, 127.8, 128.6, 129.0, 133.8, 134.6, 138.0, 139.2, 144.4 (Ar, C═N), 153.7 (C−O). $^{29}$Si NMR ($CDCl_3$): $\delta$ −74.1. Anal. Calcd for $C_{18}H_{16}N_2O$: C, 71.02; H, 5.30; N, 9.20. Found: C, 71.10; H, 5.56; N, 9.70.

**Acknowledgment.** This work was financially supported by the German Chemical Industry Fund.

**Supporting Information Available:** Crystallographic data for **1**, **2**, and **3** (in CIF format as well as tables of structure data collection and refinement details, bond lengths, angles, and torsion angles as well as atomic parameters in PDF format) and the optimized atomic coordinates of a molecule of compound **2** are available free of charge via the Internet at http://pubs.acs.org.

OM060869B

(27) Frisch, M. J.; Trucks, G. W.; Schlegel, H. B.; Scuseria, G. E.; Robb, M. A.; Cheeseman, J. R.; Montgomery, J. A., Jr.; Vreven, T.; Kudin, K. N.; Burant, J. C.; Millam, J. M.; Iyengar, S. S.; Tomasi, J.; Barone, V.; Mennucci, B.; Cossi, M.; Scalmani, G.; Rega, N.; Petersson, G. A.; Nakatsuji, H.; Hada, M.; Ehara, M.; Toyota, K.; Fukuda, R.; Hasegawa, J.; Ishida, M.; Nakajima, T.; Honda, Y.; Kitao, O.; Nakai, H.; Klene, M.; Li, X.; Knox, J. E.; Hratchian, H. P.; Cross, J. B.; Adamo, C.; Jaramillo, J.; Gomperts, R.; Stratmann, R. E.; Yazyev, O.; Austin, A. J.; Cammi, R.; Pomelli, C.; Ochterski, J. W.; Ayala, P. Y.; Morokuma, K.; Voth, G. A.; Salvador, P.; Dannenberg, J. J.; Zakrzewski, V. G.;Dapprich, S.; Daniels, A. D.; Farkas, M. C.; Strain, O.; Malick, D. K.; Rabuck, A. D.; Raghavachari, K.; Foresman, J. B.;Ortiz, J. V.;Cui, Q.; Baboul, A. G.; Clifford, S.; Cioslowski, J.; Stefanov, B. B.; Liu, G.; Liashenko, A.; Piskorz, P.; Komaromi, I.; Martin, R. L.; Fox, D. J.; Keith, T.; Al-Laham, M. A.; Peng, C. Y.; Nanayakkara, A.; Challacombe, M.; Gill, P. M. W.; Johnson, B.; Chen, W.; Wong, M. W.; Gonzalez, C.; Pople, J. A. *Gaussian03*; Gaussian Inc.: Wallingford, CT, 2004.

(28) Bieger, W.; Seifert, G.; Eschrig, H.; Grossmann, G. *Chem. Phys. Lett.* **1985**, *115*, 275.

(29) Malkin, V. G.; Malkina, O. L.; Salahub, D. R. *Chem. Phys. Lett.* **1993**, *204*, 80.

(30) Kutzelnigg, W. *Isr. J. Chem.* **1980**, *19*, 193.

(31) Kutzelnigg, W.; Fleischer, U.; Schindler, M. In *NMR Basic Principles and Progress*; Diehl, P., Fluck, E., Günther, H., Kosfeld, R., Seelig, J., Eds.; Springer: Heidelberg, 1990; Vol. 23, pp 165−262.

(32) Köster, A. M.; Geudtner, G.; Goursot, A.; Heine, T.; Vela, A.; Patchkovskii, S.; Salahub, D. R. *deMon*; NRC, Canada, 2002.

(33) (a) Foster, J. M.; Boys, S. F. *Rev. Mod. Phys*. **1960**, *32*, 296. (b) Foster, J. M.; Boys, S. F. *Rev. Mod. Phys*. **1960**, *32*, 303. (c) Foster, J. M.; Boys, S. F. *Rev. Mod. Phys.* **1960**, *32*, 305.